Heteropolynuclear lanthanide(III) complexes for cooperative sensitization upconversion in water

Léna Godec,[a] Richard C. Knighton,[a,b] Nadège Hamon,[c] Waygen Thor,[a,d] Ka-Leung Wong,[d] Raphaël Tripier,[c,*] and Loïc J. Charbonnière,[a,*]

[a] Equipe de synthèse pour l'analyse (SynPA), IPHC, UMR 7178, CNRS/Université de Strasbourg, ECPM, 25 rue Becquerel, 67087 Strasbourg Cedex, France. E-mail: l.charbonn@unistra.fr

[b] School of Chemistry and Chemical Engineering, University of Southampton, Southampton, SO17 1BJ, UK.

[c] Univ Brest, UMR CNRS 6521 CEMCA, 6 avenue Victor le Gorgeu, 29200 Brest, France.

[d] HK

KEYWORDS. Lanthanide, Molecular upconversion, luminescence, cooperative sensitization.

ABSTRACT: We report the synthesis of a tritopic ligand $\mathbf{L^2}$, composed of two strongly binding lanthanide (Ln^{3+}) sites using tris-functionalized triazacyclononane (tacn) scaffolds, bridged by a weaker Ln^{3+} binding triethylene glycol chain sites. Coordination chemistry of Ln^{3+} (Ln = Eu, Tb, Yb and Lu) was thoroughly investigated using NMR and photoluminescent spectroscopies. For all Ln^{3+} studied, the first two Ln ions are coordinated by the tacn scaffolds to form [Ln$\mathbf{L^2}$] and [$Ln_2\mathbf{L^2}$] species, followed by higher order (tri- and tetranuclear) complexes, [Ln($Ln_2\mathbf{L^2}$)] and [Ln_2($Ln_2\mathbf{L^2}$)], respectively. The third and fourth exo-macrocyclic binding events occur at the weak polyethylene glycol binding site, buttressed by a concomitant synergistic interaction of the tacn phosphonate arms, confirmed by DFT modeling of the complexes. Owing to the strong coordination of the two first cations, [$Ln_2\mathbf{L^2}$] (Ln = Tb, Eu, Yb and Lu) homobimetallic complexes were prepared and characterized (^{1}H- and ^{31}P{^{1}H}-NMR, elemental analysis and ES/MS spectrometry). The spectroscopic properties of the dinuclear species (absorption, excitation, luminescence, luminescence quantum yields and excited state lifetimes) were determined in H_2O and D_2O, revealing coordinative saturation of the Ln ions in the cavity of the tacn scaffolds (q-value ≈ 0). UV-vis and luminescence titrations of the [$Tb_2\mathbf{L^2}$] complex by addition of Eu salts in buffered water confirmed the formation of the [Eu($Tb_2\mathbf{L^2}$)] and [Eu_2($Tb_2\mathbf{L^2}$)] species, exhibiting energy transfer from Tb→ Eu downshifting. Further titration of the [$Yb_2\mathbf{L^2}$] dinuclear complex by Tbsalts in D_2O also confirmed the formation of the tri- and tetranuclear species. Upon excitation into the $^2F_{5/2} \leftarrow {}^2F_{7/2}$ absorption band of Yb at 980 nm, a cooperative sensitization upconversion process is evidenced, observating visible Tb emission bands, ($^5D_4 \rightarrow {}^7F_J$ (J = 6 to 3)). Interestingly, heating resulted in Ln scrambling in the tacn coordination sites, as evidenced by ES/MS spectrometry, increasing UC efficiency by *ca.*10^3. Surprisingly, the most efficient emitter for UC is the tetranuclear [TbYb(TbYb$\mathbf{L^2}$)] species, with one of each Ln species in the tacn scaffolds, and one of each Ln species coordinated by the polyethylene glycol chain. Further optimization on the pD of the solution led to an overall 9.0×10^{-5} % UC quantum yield (λ_{exc} = 980nm, P = 10.8 W.cm^{-2}). The same experiment was repeated in water, affording UC at the molecular level.

Upconversion (UC) consists of piling up the energy of two or more photons in a compound so that the total energy can be restored as a photon of higher energy than the excitation light.[1] While routinely documented for solid state compounds,[2] for nanoparticles,[3,4] or for mixtures of dyes in organic solvents in the case of triplet-triplet annihilation,[5] examples of discrete molecules exhibiting UC are still scarce in the literature.[6-9]

Because of their ladder like energy level and their long-lived excited states,[10] Ln^{3+} ions are prototypical elements for the construction of UC devices. However, at the molecular level, the vibrations of OH, CH and NH oscillators present in the framework of the ligands coordinated to the lanthanides or in the neighboring solvent molecules strongly quenchthe luminescence of lanthanide excited states,[11] especially for intermediate excited states situated in the near infrared (NIR) spectral domain.[12]

Despite these challenges, molecular UC has made significant progresses in the UC efficiency since the pioneering work of Piguet and coworkers on the development of supramolecular triple stranded heterotrinuclear Cr_2Er helicates.[13] While Er complexes have been shown to be efficient UC molecules in organic solvents,[14] or in D_2O[15] mainly through excited state absorption (ESA) mechanism,[16] other sources of improvements have been found in the use of polynuclear cluster complexes (also called molecular aggregates),[17-21] in metal-to-metal[22-25] or ligand-to-metal energy transfer UC (ETU),[14,26] or in the use of cooperative luminescence (CL)[27] and cooperative sensitization (CS) mechanisms.[17] CS is a specific case of UC in which two excited donor atoms simultaneously transfer their energy to a third one. The

prototypical example combines two excited Yb atoms simultaneously transferring their energy to a Tb atom, without any intermediate excited state located on the Tb acceptor.[28-30] CS was also demonstrated with *d*-transition metals (*e.g.* Ir,[31] Cr,[32] or Ru[33]) or organic ligands[34,35] as acceptors. Cooperative processes (for emission or absorption)[36,37] are of second order, contrasting with ESA or ETU, and are expected to be less efficient by several orders of magnitude.[1] However, despite the supposed inefficiency of cooperative processes, CS was shown to be comparable to other mechanisms at the molecular scale, exhibiting the only known example of UC in water for an electrostatically stabilized supramolecular assembly.[38] This success relies largely on the fact that the intermediate excited state - typically Yb in CS UC - displays a relatively long excited state lifetime of few µs,[39] whereas ESA or ETU based system implicate other lanthanide elements such as Er[18] or Ho,[40] with far shorter intermediate and final excited state lifetimes.[41] Despite the currently modest UC efficiencies of molecular based UC devices, there is great interest to iterate and improve them. UC devices benefit from a very sensitive and almost background free luminescence signals, as a result of the anti-Stokes process, particularly appealing for diagnostics[42] or microscopy imaging,[43] and because the use of nanoparticles in UC devices is beset by stability,[44,45] reproducibility and toxicity issues.[46] We have recently demonstrated that small anionic mononuclear Yb^{3+} complexes can self-assemble in the presence of Tb^{3+} cations in aqueous solutions to form Tb/Yb supramolecular heteropolynuclear assemblies,[47-49] that displayed CS UC. Linking two such Yb complexes by a bridge containing a third coordination site for the introduction of the Tb cation allows to encode a further step in the controlled formation of the polynuclear complexes. This builds on our prior art which ultimately led to the hierarchical formation of controlled Yb/Tb heterpolynuclear complexes. Considering the very similar chemical behavior of Ln^{3+} cations along the series, a strict control of the position of the different Ln^{3+} cations can hardly be obtained on the basis of the ionic radii alone.[50] Alternative approaches rely on a step by step chemical assembly of pre-formed complexes,[51] stepwise deprotection of the coordinating sites,[52] or thermodynamically induced site selective coordination.[53] We chose this latter approach by playing with the hard coordination sites on the phosphonate functions anchored on two triazacyclononane (tacn) moieties - for the introduction of the two first Ln^{3+} cations - while the third coordination will be ensured by the softer oxygen atoms present on a polyethylene glycol chain.[54] However, Significant synthetic effort is required to obtain such pre-organized ligands, and our recent findings have shown that the choice of the linker is crucial, as it can induce rigidity or length constraints that may negatively impact the expected upconversion (UC) efficiency.[55]

We here present the synthesis and coordination behavior of a tris-heteropolytopic ligand **L²** (Chart 1), based on two pyridyl functionalized triazacyclonane (tacn) lateral coordinating platforms bridged by a weakly coordinating polyethylene glycol chain. The selection of the two different coordinating sites, was guided by the formation of highly stable Ln complexes with the tacn-phosphonated ligands, as previously demonstrated with an analogue of **L¹**,[56] and by the weaker coordinating ability of polyethylene glycol chains.[57-59] The introduction of a additional coordinating linker significantly improves the UC efficiency, now enabling CS UC in pure water.

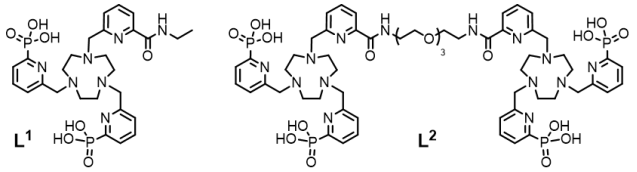

Chart 1. Hetero-tritopic ligand L² and its monotopic analogue L¹.[56]

Results and discussion

Synthesis of **L²**. The convergent synthesis of ligand **L²** involves reaction between the tacn platform (**5**) and the bis(chloromethylpicolinamide)triethyleneglycol bridge as depicted in Scheme 1. The tacn moieties **5** are first obtained by the *N,N*-dialkylation using 6-ethylphosphonic-2-chloromethylpyridine, previously described in the preparation of the monotopic analogue **L¹**.[56]

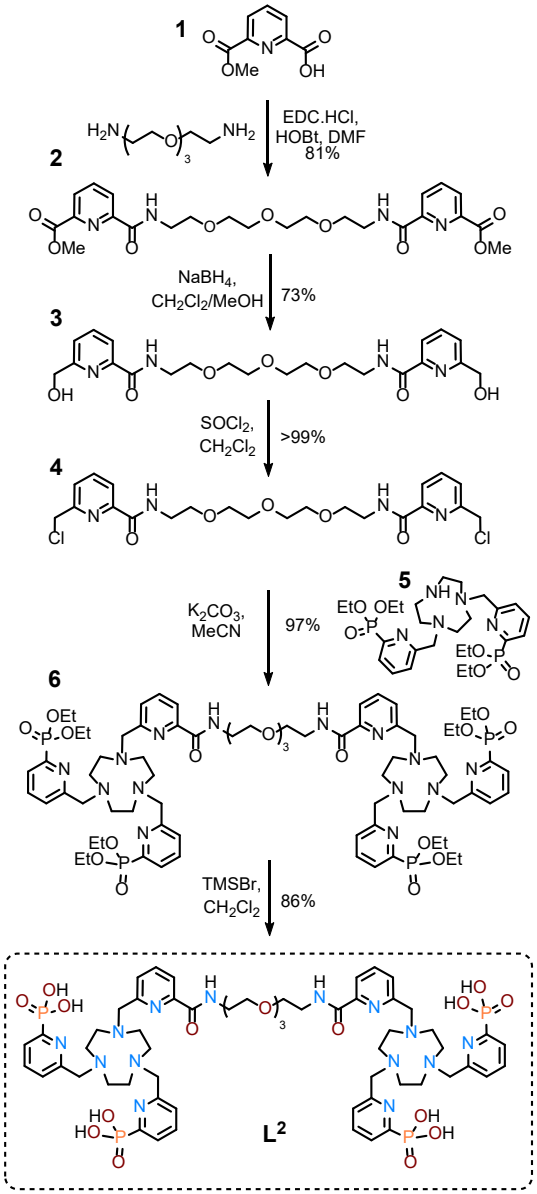

Scheme 1. Synthesis of ligand L².

In parallel, activation of the acid function of compound **1**[60] enables its coupling to the amine terminated tetraethylene glycol, affording the diamide **2**. Selective reduction of the terminal esters with $NaBH_4$, followed by chlorination with $SOCl_2$, led to the alcohol **3** and its chlorinated derivative **4**, respectively. Reaction of **4** with the bis-substituted tacn precursor **5** affords the protected ligand **6**, which is subsequently deprotected using TMSBr in dichloromethane, followed by solvolysis, to afford ligand **L²**. Full experimental synthetic details can be found in the Supplementary Information section.

Coordination behavior of L² with Ln^{3+} cations. To investigate the coordination behavior of **L²** with trivalent Ln cations, titration experiments were conducted by incrementally adding Ln cations and monitoring the resulting mixture by UV-Vis absorption spectroscopy, luminescence spectroscopy or ^{1}H- and ^{31}P{^{1}H}NMR spectroscopy.

Spectrophotometric titration of L² by Eu, Tb and Yb. Figure 1 displays the evolution of the UV-Vis absorption and luminescence spectra of the solution of **L²** upon addition of $EuCl_3$ salts.

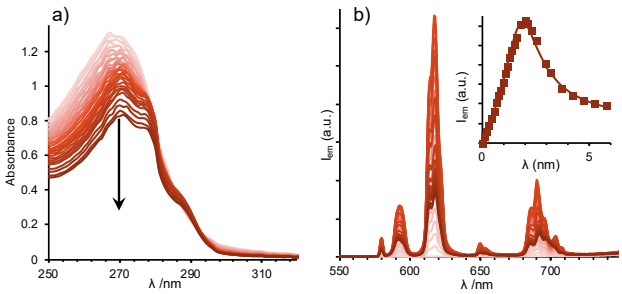

Figure 1. a) Evolution of the UV-Vis absorption spectra and b) of the emission spectra (λ_{exc} = 268 nm) of a 4.3×10^{-6} mol.L^{-1} solution of **L²** upon addition of a solution of $EuCl_3.6H_2O$ (10 mM TRIS/HCl buffer, pH 7.3). Inset: Evolution of the overall emitted intensity (squared dots) and fitted data (red line).

The UV-Vis absorption spectra of the ligand iscomposed of a broad absorption band with maximum at 268 nm corresponding to π→π* transitions centered on the pyridyl rings. Upon addition of the Eu^{3+} salt from 0.0- 2.0 equivalents, the absorption spectra display a small bathochromic shift to 271 nm, and the appearance of vibronic structure indicating rigidification of the tacn moieties, attributed to the complexation of the Eu^{3+} cations within the tacn cavity and the concomitant wrapping of the pyridyl arms upon coordination. After two equivalents, no further change could be observed in the UV-Vis absorption spectra. Concerning the luminescence spectra, the addition of Eu^{3+} immediately resulted in the observation of the characteristic emission spectra of Eu upon excitation into the ligand absorption band (λ_{exc} = 268 nm), corresponding to the $^5D_0 \rightarrow {}^7F_J$ (J = 0 to 4) electronic transitions centered on Eu in the region going from 580 to 720 nm. [10] The Eu centered luminescence gradually increased up to two equivalents of Eu^{3+}, however, in contrast to the absorption data, further additions of salts above two equivalents led to a strong decrease of the luminescence intensity accompanied by a change of the shape of the spectra, particularly in the region of the $^5D_0 \rightarrow {}^7F_4$ electronic transition from 680 to 715 nm. The sharp maximum observed at two equivalents of added salts (Figure 1c) was indicative of the strong affinity of the two first cations with the ligands. Altogether, these results indicate the formation of at least three species. The first two one correspond to the coordination of one and two Eu^{3+} cations within the tacn moieties, as evidenced by UV-Vis variations and the appearance of a strong luminescence signal. addition of further Eu^{3+} cations leads to a decrease in luminescence intensity, attributed to these supplementary cations being less shielded from surrounding water molecules and thus more susceptible to luminescence quenching. The data were analyzed according to previously published procedures[61] using the Specfit software.[62,63] An excellent fit was obtained using a model comprising the formation of four successive [Eu_x**L²**] species (x = 1 to 4), but as mentioned above, the very strong coordination of the two first cations precludes the exact determination of the associated stability constants. A speciation diagram representing the calculated evolution of the species formed in solution and the calculated emission spectra of the species are presented in Figure S29. The same behavior was observed for the titration of **L²** with Tb^{3+} (Figure S30). In contrast, upon titration with the smaller Yb^{3+} cation, the highest luminescence intensity was first observed at a lower Yb^{3+}/**L²** ratio than two (Figure S31a). This behavior is readily explained by the significantly slower kinetics of complexation. Batch experiments, in which the mixtures were monitored over several days under heating (Figure S31b), finally showed the same behavior as observed for the lighter Eu^{3+} and Tb^{3+} cations.

Titration of L² by Lu^{3+} followed by ^{1}H- and ^{31}P{^{1}H}-NMR spectroscopy. The interaction of **L²** with the small Lu^{3+} cation (ionic radii = 0.977 Å for a coordination number of 8)[64] with broad and ill-defined peaks being observed immediately after the addition of Lu aliquots. However, heating the samples to 60°C for one hour allowed equilibration of the system and observation of narrow signals. Figure 2 displays the evolution of the ^{1}H-NMR spectra during the titration experiment.

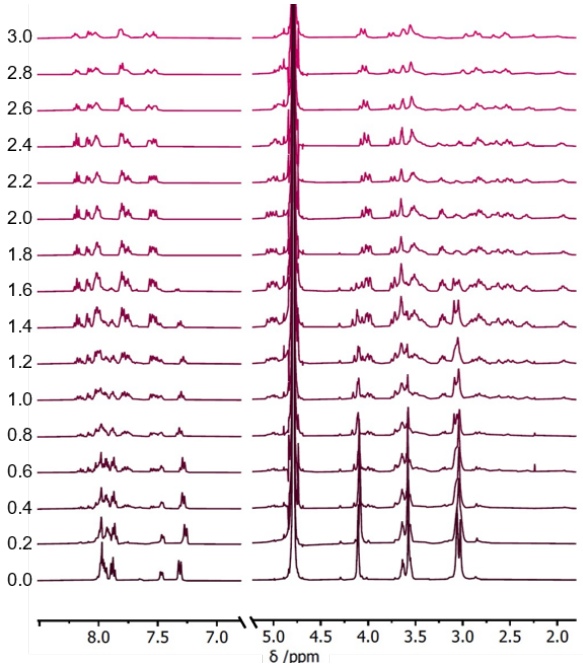

Figure 2. ^{1}H NMR spectra of ligand **L²** upon addition of 0-3 equiv. of $LuCl_3{\cdot}6H_2O$ (D_2O, pD = 7.0, 298 K, 400 MHz).

The complexation was evidenced by NMR, with a progressive disappearance of the peaks of the free ligand, a general downfield shift of the signals of the aromatic proton atoms up to two equivalents, and a complexification of the patterns in the aliphatic region, with appearance of new peaks characteristics of the coordination of the Lu^{3+} cation in the cavity of the tacn moiety such as those of the methylene groups between 1.8 and 3.0 ppm. The spectra gradually evolved up to two equivalents, but no significant shifts were observed between 2.0-3.0 equivalents, except for an increased broadening of the signals. The titration was also monitored by $^{31}P\{^1H\}$-NMR spectroscopy (Figure 3). From 0.0-2.0 equivalents, one can observe the disappearance of the single peak of the phosphorus atom of the phosphonic functions at *ca.* 4.8 ppm, while two new peaks emerged around 12 and 13 ppm.

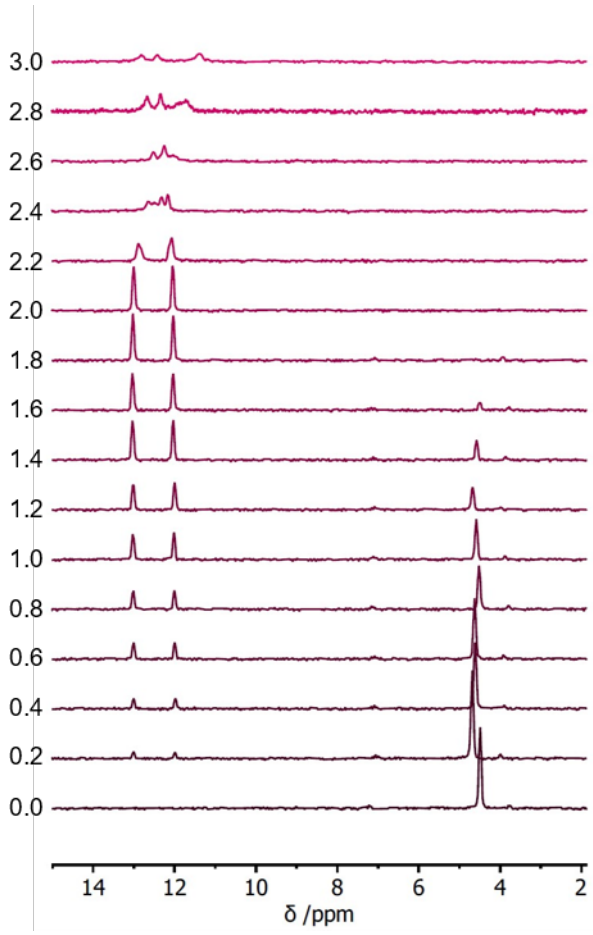

Figure 3. $^{31}P\{^1H\}$-NMR spectra of ligand **L²** upon addition of 0.0-3.0 equiv. of $LuCl_3 \cdot 6H_2O$ (D_2O, pD = 7.0, 298 K, 162 MHz).

The splitting into two signals is a clear evidence of the coordination of the Lu^{3+} cation into the cavity of the tacn platform, resulting in the wrapping of pyridyl arms around the metal, with a pseudo-C_3 symmetry around Lu^{3+} and a loss of the equivalence of the two phosphonate functions from the free ligand to the complex. This is a salient point as it results from the formation of Δ and Λ isomers at each lateral coordination site, meaning the formation of pairs of diastereoisomers for the dinuclear complexes (ΔΛ and ΔΔ, and ΛΔ and ΛΛ). Although one might expect up to four new peaks in the ^{31}P-NMR spectrum, the distances between the lateral coordinating sites observed in the DFT modeling (*vide infra*) results in a weak influence of one coordinating site on the other and chemical shifts which are isochronous for the two diastereisomers. The presence of these diastereoisomeric pairs may also result in different coordination behaviors for the next Ln^{3+} to be incorporated into the structure. Above two equivalents of added cation, the signals broadened and split to four dinstinct peaks, mirroring the different coordination of the incoming Lu^{3+} cation with the two diastereoisomeric forms of the dinuclear complexes.

DFT modelling of the polynuclear species. Despite our repeated efforts to getcrystals of the complexes suitable for X-ray diffraction analysis, those remained unsuccessful and we turned our attention towards DFT modeling to get insights into the structural behavior of the complexes (Figure 4).

The model obtained for the dinuclear [Ln_2**L²**] complex agrees with the coordination of the Ln^{3+} cations in the cavity of the tacn coordination sites, as it was also evidenced by NMR spectroscopy and excited state lifetime measurements on the dinuclear complexes (*vide infra*). Assuming deprotonation of all phosphonate functions, each lateral complex will be negatively charged and will repel each other, resulting in the polyethylene glycol chain to be fully extended, positioning the two Ln^{3+} cations at 20.8 Å one from the other. Modelling both ΔΔ or ΔΛ diastereoisomers showed no statistically signiciant energy difference between them. Introduction of the third Ln^{3+} cation resulted in the contraction of the overall architecture, with the coordination of the incoming cation by only two of the three oxygen atoms of the PEG chain, and additional coordination of the two phosphonate functions of each lateral complex, one of the four phosphonate function being coordinated by two of its O atoms, resulting in an heptadentate coordination of the central Ln^{3+} cation. This coordination mode is similar, whatever the starting diastereoisomeric pair modeled (ΔΔ or ΔΛ). Interestingly, the lateral site coordinating the central Ln^{3+} by three O atoms of the phosphonate functions (named Ln1) is on the same side as the O atom of the PEG chain which is not coordinated to the central Ln^{3+} (named Ln2, Ln3 representing the lateral site coordinated by only two O atoms of the phosphonate functions). The Ln2-Ln3 distances are similar for both diastereosomeric forms ($d_{Ln2\text{-}Ln3}$ = 5.19 Å). In contrast, $d_{Ln1\text{-}Ln2}$ is shorter for the ΔΔ isomer (4.67 Å) compared to the ΔΛ one (4.86 Å), but the Ln1-Ln3 distances are almost identical for both (9.80 for ΔΔ, 9.83 Å for ΔΛ) as a result of a smaller Ln1-Ln2-Ln3 angle for the ΔΛ isomer (respectively 154° and 170° for ΔΛ and ΔΔ).

Figure 4. DFT models of the di-, tri- and tetranuclear complexes of Ln^{3+} with ligand **L²**.

Synthesis and characterization of the Ln-dinuclear complexes (Ln = Eu^{3+}, Tb^{3+}, Yb^{3+} and Lu^{3+}). Considering that the coordination within the tacn cavity affords stable complexes that can be isolated and purified, the complexes were synthesized and fully characterized by ^1H- and ^{31}P-NMR spectroscopy (except for Tb for which the paramagnetic contribution rendered the spectra uninterpretable), electrospray mass spectrometry (ES/MS) and elemental analysis (See Supplementary Information). In all cases, the ES/MS spectra were fully

consistent with the expected [Ln_2**L²**] compositions, particularly with respect to the isotopic distribution (Figure S20, S22, S25 and S28). An interesting feature of the $^{31}P\{^1H\}$-NMR of the paramagnetic Eu^{3+} and Yb^{3+} complexes was the presence of two sets of two peaks, corresponding to the presence of the diastereoisomers. For both Eu^{3+} and Yb^{3+}, the strong paramagnetic contribution of the cations resulted in a broader dispersion of the chemical shifts, [65] allowing each environment to be distinguished in the spectra.

The spectroscopic properties were then determined for the luminescent Tb, Eu and Yb complexes in H_2O and D_2O and the main properties are gathered in Table 1, while absorption, excitation and emission spectra are compiled in Figure 4. The absorption spectra are very similar with an absorption maxima at 270 nm, corresponding to $\pi \rightarrow \pi^*$ transitions centered on the pyridyl rings. Whatever the Ln, excitation of the complexes into these absorption band revealed the atomic like emission spectra of the corresponding Ln atoms[10] with the $^5D_4 \rightarrow {}^7F_J$ (J = 6 to 2, at respectively 485, 545, 586 and 616 nm) electronic transitions of Tb, the $^5D_0 \rightarrow {}^7F_J$ (J = 0 to 4 at respectively 575, 585, 615, 650 and 670-700 nm) for Eu and a broad band centered around 980 nm for the $^2F_{5/2} \rightarrow {}^2F_{7/2}$ transition of Yb (Figure 6).

Table 1. Main Spectroscopic Parameters of the [Yb_2L²**], [Tb_2**L²**] and [Eu_2**L²**] Complexes in H_2O and D_2O at pH = 7.2.**

	λ_{exc} nm	ε_{H2O} M-1.cm-1	ϕ_{H2O} %	ϕ_{D2O} %	τ_{H2O} µs	τ_{D2O} µs	q[d]
[Eu_2**L²**]	270	27 340	11[a]	17[a]	1195	1753	0
[Tb_2**L²**]	270	25 360	49[b]	51[b]	2488	2675	-0.1
[Yb_2**L²**]	270	27 790	0.17[c]	0.7[c]	3.8	10.5	-0.1

a) Using [Ru(bipy)$_3$]Cl_2 in water (ϕ = 4 %) as a reference.[66] b) Using Rhodamine 6G in water (ϕ = 76 %) as a reference.[67] c) Using indocyanine green (ϕ = 7.8 %) as a reference.[68] d) calculated according to ref 12.

Recording the excitation spectra of the complexes upon emission at their maximum of emission typically showed the UV excitation corresponding to the UV-Vis transitions of the ligand, evidencing the antenna effect with energy transfer from the ligand to the Ln excited states.[69] From the excited state lifetimes determined in both H_2O and D_2O and using the methodology developed by Horrocks[70] and further refined by Beeby,[12] one can determined that the first coordination sphere of the Ln cations is fully saturated by the coordination of the nonadentate sites with no water molecules in the first coordination sphere and a good protection of the cations in the cavities. In the case of Yb^{3+}, this observation confirms the inclusion of the cation in the cavity, despite the slow kinetics of complexation. The luminescence quantum yields of the complexes are in line with those obtained with other ligands based on pyridyl phosphonate[48-49] or pyridyl carboxylate functions.[71]

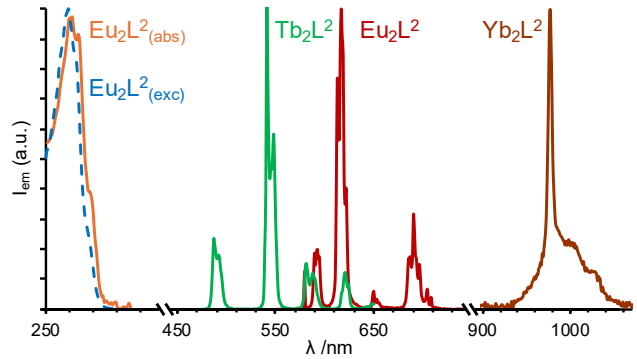

Figure 6. UV/vis absorption (orange) and excitation (blue) spectra of [Eu_2**L²**] (left) and normalized emission spectra (λ_{exc} = 270 nm) of a H_2O solution of [Ln_2**L²**] with Ln = Yb (brown), Eu (red) and Tb (green) (right).

For the Eu^{3+} complex, a luminescence spectroscopic titration was performed by monitoring the luminescence intensity as a function of the pH of the solution (Figure S32). A *pK* value of 7.2 was determined from the large increase in intensity observed below pH 8.0. This value is consistent with the second deprotonation of the phosphonate functions,[72,73] indicating that the [Eu_2**L²**]$^{2-}$ species is the predominant form above pH 7.2.

Spectrophotometric titration of [Tb_2Ln²] by Eu^{3+}. In order to better understand the coordination of the additional Ln^{3+} atoms in the polynuclear species spectroscopic titrations were performed in which the dinuclear Tb^{3+} complex was titrated by increasing amounts of $EuCl_3.6H_2O$ salts, the solution being monitored by luminescence spectroscopy. Figure 7 represents the evolution of the emission spectra as a function of the number of equivalents of added Eu^{3+} equivalents.

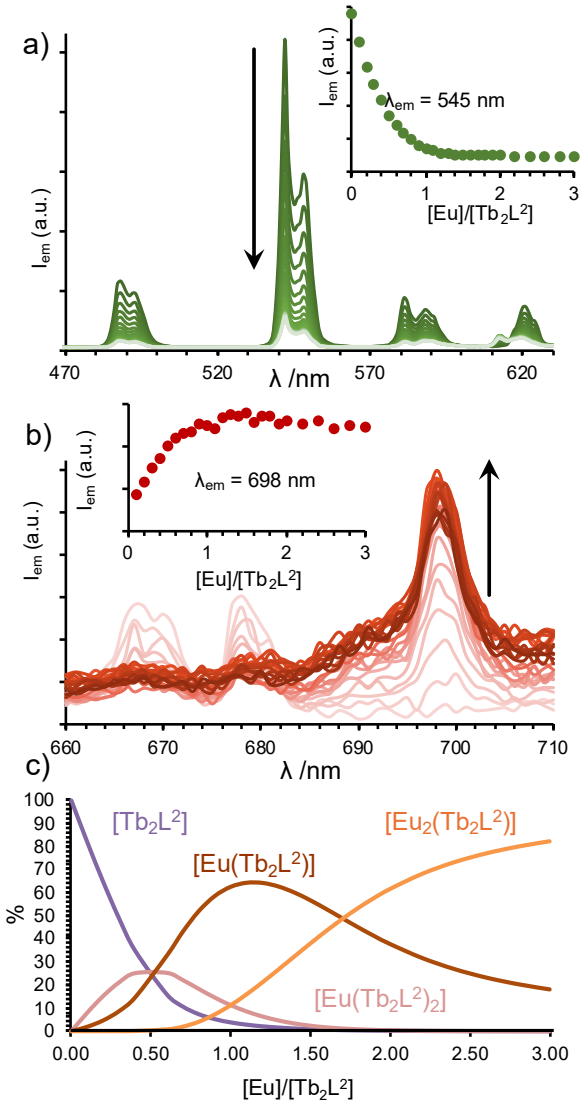

Figure 7. (a) Evolution of the intensity of luminescence of a [Tb$_2$**L^2**] solution upon addition of Eu^{3+} ([Tb$_2$**L^2**] = 1.9x10-5 M, pH = 7.0, TRIS/HCl 0.01 M, λ_{exc} = 270 nm), (b) enlargement of the 660-720 nm region and (c) speciation diagram obtained from the fitting of the titration (charges are omitted for clarity).

Addition of Eu^{3+} to the solution immediately led to the decrease of the emission of Tb^{3+}, with the concomitant observation of weak emission peaks of Eu at 616 nm ($^5D_0 \rightarrow {}^7F_2$ transition) and *ca.* 700 ($^5D_0 \rightarrow {}^7F_4$ transition) nm. The enlargement of the region between 660 and 720 nm (Figure 7b) revealed that this emission is very weak as the $^5D_0 \rightarrow {}^7F_4$ transition of Eu at 700 nm is almost of the same intensity as the very weak $^5D_4 \rightarrow {}^7F_{1,0}$ transitions of Tb at 670 and 678 nm, respectively. This behavior was attributed to an energy transfer from the Tb excited state to the Eu atoms,[74] occurring due to the overlap between the $^5D_4 \rightarrow {}^7F_4$ emission band of Tb from 570 to 700 nm and the $^5D_0 \rightarrow {}^7F_0$ absorption of Eu at 575 nm. Fitting of the data with the non-linear least-squared analysis of the Specfit software,[62-63] could be realized with a model containing three new species (Figure 7c). Apart from the expected [Eu(Tb$_2$**L^2**)] and [Eu$_2$(Tb$_2$**L^2**)] species, as previously observed for the titrations of **L^2** with Eu^{3+}, Tb^{3+} or Yb^{3+} (*vide supra*), an intermediate complex made of a single Eu^{3+} atoms coordinated to two [**Tb^2**Ln$_2$] entities could be evidenced. However, the observation of this species should be interpreted with caution, as its detection relies primarily on the evolution of the Eu bands, which are significantly weaker than those of Tb ones.

Titration of [Yb$_2$Ln^2] by Tb^{3+}. Comforted by the observation of the heteropolynuclear complexes of Eu and Tb, we turned our attention to the case of a titration of [Yb$_2$**L^2**] by Tb^{3+}, with the aim to observe UC in these complexes. The first experiment was a titration of a D_2O solution of [Yb$_2$**L^2**] by increasing amounts of $TbCl_3.6H_2O$ in D_2O, the pD of the solution being constant at 7.3 using diluted DCl when necessary during the titration. The emission spectra of Tb in the visible region was then monitored upon laser excitation into the $^2F_{5/2} \leftarrow {}^2F_{7/2}$ absorption band of Yb at 980 nm. Initial titration studies (Figure 8a) appeared ominous, exhibiting a very weak UC intensity. Considering that the titration of **L^2** by Yb^{3+} (vide supra) had revealed slow kineticss, we again utilized batch experiments. Measuring the spectra five minutes after the preparation of each batch led to the same observation (Figure S33). However, upon heating, the UC emission intensity gradually increased and finally reached a plateau after 10 days of heating at 60°C (Figure 8b), with an impressive gain of almost three orders of magnitude. Notwithstanding, the maximum of UC emission was observed for two equivalents of added Tb^{3+}, *i.e.* a one to one Yb to Tb ratio, as previously observed for other CS UC phenomena in D_2O,[27] and which is explained better as a cooperative rather than an accretive UC mechanism.[75,76] Above three equivalents, there was a deleterious effect on the UC intensity which was largely absent once four equivalents had been reached.

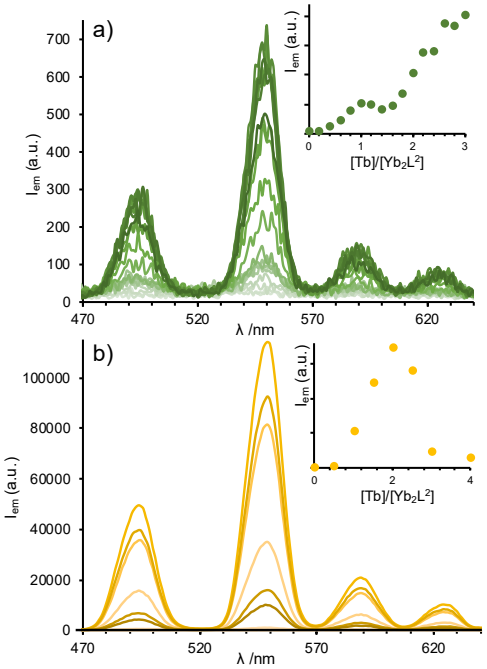

Figure 8. (a) Emission spectra measured during titration with $TbCl_3.6H_2O$ of a 1.01 mM solution of [Yb$_2$**L^2**] in D_2O (λ_{exc} = 980 nm, P_{980} = 1.08 W, 10 scans). Inset: Evolution of the emission intensity as a function of the [Tb^{3+}]/[Yb$_2$**L^2**] ratio. (b) Emission spectra measured for batches of a solution of [Yb$_2$**L^2**] in D_2O with different amount of $TbCl_3.6H_2O$, after 10 days at 60°C (λ_{exc}

= 980 nm, P_{980} = 1.08 W, 10 scans). Inset: Evolution of the emission intensity as a function of the $[Tb^{3+}]/[Yb_2\mathbf{L^2}]$ ratio.

In order to confirm the UC process, the Log/Log plot, representing the UC emission intensity as a function of the power density of the laser at 980 nm in a logarithmic scale, was recorded for the solution with two equivalents of Tb^{3+} heated for 10 days at 60°C (Figure 9). Fitting of the data with a linear regression gave a very good fit (R = 0.998), with a slope of 1.96, very close to the slope of two expected for a two-photon process such as UC.[77] The intensity of UC of this solution was also optimized relative to the pD of the solution, demonstrating another two-fold increase of the UC intensity on going from pD 7.0 to 8.5 (Figure S34).

Finally, the UC quantum yield (QY) was determined according to previously published procedures (see SI for full experimental procedure)[38] and a value of $9.0(1.8)\times10^{-7}$ was obtained (pD = 8.6, P_{980} = 1.08 W), which is 64 times higher for this molecular system compared to previous supramolecular assemblies.

However, prolonged heating the solution may significantly impact the system by inducing cation scrambling and exchange within the tacn macrocyclic cavities.. To test this hypothesis, electrospray mass spectrometry was employed as a method of choice. Figure S35 represents the ES/MS spectrum of a solution of the dinuclear Yb complex containing two equivalents of Tb^{3+} five minutes after their mixing. In the negative mode, two major peaks are observed: one corresponding to the dianionic $[Yb_2\mathbf{L^2}]^{2-}$ centered around 853.65 *m/z* units and the singly charged anion $[Yb_2\mathbf{L^2}H]^-$ anion at 1707.29 *m/z*.[78] No evidence of the tri- and tetranuclear complexes was observed.

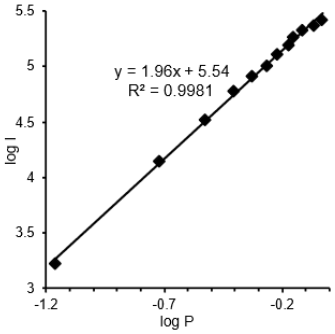

Figure 9. Log-log plot of Tb emitted intensity at 545 nm versus laser excitation intensity at 980 nm for a 1.06 mM solution of $[Yb_2\mathbf{L^2}]$ in D_2O containing two equivalents of $TbCl_3.6H_2O$ (λ_{exc} =980 nm) after 10 days at 60°C.

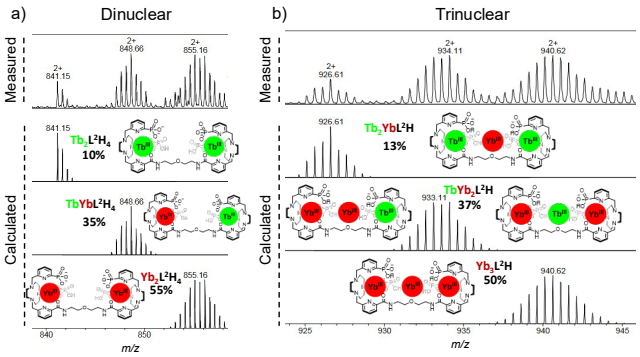

Figure 10. ES/MS⁺ spectra of an aqueous solution containing $[Yb_2\mathbf{L^2}]$ complex and two equivalents of $TbCl_3.6H_2O$ after one month at 60°C expanded on the region of the dinuclear $[Ln_2\mathbf{L^2}H_4]^{2+}$ species (a) and the trinuclear $[Ln_3\mathbf{L^2}H]^{2+}$ species (b). The lower parts correspond to the calculated spectra.

The same solution was injected after being heated at 60°C for one month (Figure 10). To improve the ES/MS response, the solution was acidified just before measurements using formic acid. After one month of heating, the region corresponding to the doubly charged dinuclear species (Figure 10, left) displayed three peaks pointing at 841.15, 848.66 and 855.16 *m/z* units, which can be attributed to the $[Tb_2\mathbf{L^2}H_4]^{2+}$, $[TbYb\mathbf{L^2}H_4]^{2+}$ and $[Yb_2\mathbf{L^2}H_4]^{2+}$ species, respectively. This observation unambiguously points to an exchange of the Ln elements within the cavity of the tacn complex. Assuming that the ionization energies are the same for the Yb and Tb containing species, integration of the isotopic distribution patterns allows for an estimation of the relative proportions of each species, corresponding respectively to 10%, 35% and 55%. Considering that the UC luminescence of such a solution has reached its equilibrium after ten days of heating (*vide supra*), one can surmise that the thermodynamic equilibrium has been reach. From this point, the standard free enthalpies for the replacement of the first and second Yb atoms by Tb ones can be calculated as 3.3 and 5.5 $kJ.mol^{-1}$ respectively (see full details in the supplementary information section). These positive values confirm that the stability constants for the complexation of Yb in the tacn cavities are higher than those of Tb, in line with the observed lower kinetics of complexation of Yb (*vide supra*), requiring heating to reach the thermodynamic equilibrium.

Interestingly, the positive ionization mode ES/MS also revealed the observation of trinuclear species corresponding to the general $[Ln_3\mathbf{L^2}H]^{2+}$ formula. It is to be noted that the relative proportions closely match those observed for the dinuclear species within experimental errors, which reflects that the coordination of the third cations is far weaker than the first two binding events. Unfortunately, no trace of the tetranuclear species could be observed.

Surprisingly, the ES/MS results indicated that the best UC signal was obtained for a trinuclear species having predominantly one Yb and one Tb cation in each of the tacn cavities. This observation is counterintuetive as it implicates the exo-tacn Yb cation as a crucial component oif the UC process, despite the fact that it is likely less protected from the water molecules and thus more prone to non-radiative deactivations.

With all these optimization steps in hands, we finally performed the experiment in non-deuterated water at pH 8.4 by first mixing a mixture of one equivalent of each Yb^{3+} and Tb^{3+} cations to one equivalent of $\mathbf{L^2}$, heated at 60°C for 30 minutes, followed by a subsequent simultaneous addition of one equivalent of Tb^{3+} and Yb^{3+}. The UC measured upon excitation at 980 nm (Figure 11). In that case, 30 scans were accumulated instead of 10 for the other experiments.

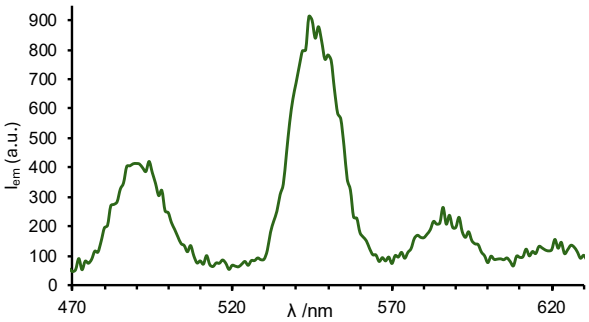

Figure 11. Emission spectrum measured when one equivalent of Yb^{3+} and one equivalent of Tb^{3+} were added simultaneously to a solution containing the 1.35 mM heteropolynuclear complex in H_2O at pH 8.4 (λ_{exc} = 980 nm, P_{980} = 1.08 W, 30 scans).

The UC emission of Tb could be obtained for the first time at the molecular scale using a single-species emitter on a heteropolynuclear Yb/Tb complex with a UC QY of $1.5(3)\times10^{-9}$. Although still extremely low compared to UC nanoparticles,[79] it is perfectly in line with other UCQY obtained for discrete molecular systems in organic solvents such as those of Er based complexes described in the literature.[80]

Conclusion

We successfully designed and synthesized a tris-heteropolytopic ligand based on azamacrocyclic-platforms, **L²**, specifically tailored for the controlled formation of heteropolynuclear lanthanidecomplexes. By leveraging the unique combination of strong coordination sites (tacn scaffolds) and weaker binding sites (polyethylene glycol chain), we have demonstrated the ability to assemble and control the composition of polynuclear lanthanide complexes in aqueous solutions. Comprehensive spectroscopic, titration, and DFT studies confirmed the stability, speciation, and structural characteristics of these complexes, providing insights, thanks to our earlier studies,[55] into the role of linker rigidity and the induced symmetry of coordination.

Most notably, we achieved cooperative sensitization UC in pure water at the molecular level, with optimized UC efficiency resulting from thermal scrambling and specific lanthanidecombinations. The highest UC intensity was observed for tetranuclear complexes with equimolar quantities of Yb^{3+} and Tb^{3+} ions, highlighting the critical role of the lanthanide configuration and their situation within the global ligand's architecture. Thanks to the ligand pre-organization enforcing close approach of the cations, the obtained UC QY displayed a 64-fold increase compared to the single example previously described in the literature for molecular systems in water.

These findings provide valuable contributions to the development of molecular UC systems, particularly for applications in bioimaging and photonic devices, where aqueous stability and efficiency remain critical challenges. While UC quantum yields remain low compared to nanoparticle systems, this work underscores the potential for further optimization of molecular systems to bridge this gap, addressing reproducibility concerns in more complex UC technologies and materials.

Finally, building on our previous work and the results presented here, we are now accumulating significant data on the design of such systems, particularly regarding the role and nature of the lateral macrocycles and the central linker. This knowledge enables us to fine-tune current systems and envision the development of even more efficient designs in the future.

ASSOCIATED CONTENT

Supporting Information. A brief statement in nonsentence format listing the contents of material supplied as Supporting Information should be included, ending with "This material is available free of charge via the Internet at http://pubs.acs.org." For instructions on what should be included in the Supporting Information as well as how to prepare this material for publication, refer to the journal's Instructions for Authors.

AUTHOR INFORMATION

Corresponding Author

Dr Loïc J. Charbonnière, Equipe de synthèse pour l'analyse (SynPA), IPHC, UMR 7178, CNRS/Université de Strasbourg, ECPM, 25 rue Becquerel, 67087 Strasbourg Cedex, France. E-mail: l.charbonn@unistra.fr

Present Addresses

†If an author's address is different than the one given in the affiliation line, this information may be included here.

Author Contributions

The manuscript was written through contributions of all authors. All authors have given approval to the final version of the manuscript.

Funding Sources

The French Agence Nationale pour la Recherche is gratefully acknowledge for financial support (LUCAS Project, ANR 19-CE29-0014-01).

ACKNOWLEDGMENT

L.J.C. and L.G. acknowledge the help of Dr Jean-Marc Strub (IPHC, UMR 7178, Strasbourg, France) for recording and interpreting ES/MS spectra.

ABBREVIATIONS

UC, up conversion; NIR, near infrared; ESA, Excited state absorption; ETU, energy transfer up conversion; CL, cooperative luminescence; CS, cooperative sensitization; tacn, triazacyclononane.

REFERENCES

(1) Auzel, F. Upconversion and Anti-Stokes Processes with f and d Ions in Solids. *Chem. Rev.* **2004**, *104* (1), 139–174.

(2) Gamelin, D. R.; Güdel, H. U. Design of Luminescent Inorganic Materials: New Photophysical Processes Studied by Optical Spectroscopy. *Acc. Chem. Res.* **2000**, *33* (4), 235–242.

(3) Zhu, X.; Su, Q.; Feng, W.; Li, F. Anti-Stokes Shift Luminescent Materials for Bio-Applications. *Chem. Soc. Rev.* **2017**, *46* (4), 1025–1039.

(4) Zhou, J.; Liu, Q.; Feng, W.; Sun, Y.; Li, F. Upconversion Luminescent Materials: Advances and Applications. *Chem. Rev.* **2015**, *115* (1), 395–465.

(5) Bharmoria, P.; Bildirir, H.; Moth-Poulsen, K. Triplet–Triplet Annihilation Based near Infrared to Visible Molecular Photon Upconversion. *Chem. Soc. Rev.* **2020**, *49* (18), 6529–6554.

(6) Bolvin, H.; Fürstenberg, A.; Golesorkhi, B.; Nozary, H.; Taarit, I.; Piguet, C. Metal-Based Linear Light Upconversion Implemented in Molecular Complexes: Challenges and Perspectives. *Acc. Chem. Res.* **2022**, *55*, 442–456.

(7) Yin, H.-J.; Xiao, Z.-G.; Feng, Y.; Yao, C.-J. Recent Progress in Photonic Upconversion Materials for Organic Lanthanide Complexes. *Materials* **2023**, *16* (16), 5642.

(8) Nonat, A. M.; Charbonnière, L. J. Upconversion of Light with Molecular and Supramolecular Lanthanide Complexes. *Coord. Chem. Rev.* **2020**, *409*, 213192.

(9) Charbonnière, L.J.; Nonat, A.M.; Knighton, R.C.; Godec, L. Upconverting photons at the molecular scale with lanthanide complexes. *Chem. Sci.* **2024**. *15*, 3048-3059.

(10) Eliseeva, S. V.; Bünzli, J.-C. G. Lanthanide Luminescence for Functional Materials and Bio-Sciences. *Chem. Soc. Rev.* **2009**, *39* (1), 189–227.

(11) Supkowski, R.M.; Horrocks, W.D.W. On the determination of the number of water molecules, q, coordinated to europium(III) ions in solution from luminescence decay lifetimes. *Inorg. Chim. Acta* **2002**, *340*, 44-48.

(12) Beeby, A.; Clarkson, I. M.; Dickins, R. S.; Faulkner, S.; Parker, D.; Royle, L.; Sousa, A. S. de; Williams, J. A. G.; Woods, M. Non-Radiative Deactivation of the Excited States of Europium, Terbium and Ytterbium Complexes by Proximate Energy-Matched OH, NH and CH Oscillators: An Improved Luminescence Method for Establishing Solution Hydration States. *J. Chem. Soc. Perkin Trans. 2* **1999**, 493–504.

(13) Aboshyan-Sorgho, L.; Besnard, C.; Pattison, P.; Kittilstved, K. R.; Aebischer, A.; Bünzli, J.-C. G.; Hauser, A.; Piguet, C. Near-Infrared→Visible Light Upconversion in a Molecular Trinuclear d–f–d Complex. *Angew. Chem. Int. Ed.* **2011**, *50* (18), 4108–4112.

(14) Taarit, I.; Alves, F.; Benchohra, A.; Guénée, L.; Golesorkhi, B.; Rosspeintner, A.; Fürstenberg, A.; Piguet, C. Seeking Brightness in Molecular Erbium-Based Light Upconversion. *J. Am. Chem. Soc.* **2023**, *145* (15), 8621–8633.

(15) Nonat, A.; Chan, C. F.; Liu, T.; Platas-Iglesias, C.; Liu, Z.; Wong, W.-T.; Wong, W.-K.; Wong, K.-L.; Charbonnière, L. J. Room Temperature Molecular up Conversion in Solution. *Nat. Commun.* **2016**, *7* (1), 11978.

(16) Golesorkhi, B.; Nozary, H.; Guénée, L.; Fürstenberg, A.; Piguet, C. Room-Temperature Linear Light Upconversion in a Mononuclear Erbium Molecular Complex. *Angew. Chem. Int. Ed.* **2018**, *57* (46), 15172–15176.

(17) Knighton, R. C.; Soro, L. K.; Francés-Soriano, L.; Rodríguez-Rodríguez, A.; Pilet, G.; Lenertz, M.; Platas-Iglesias, C.; Hildebrandt, N.; Charbonnière, L. J. Cooperative Luminescence and Cooperative Sensitisation Upconversion of Lanthanide Complexes in Solution. *Angew. Chem. Int. Ed.* **2022**, *61* (4), e202113114.

(18) Gálico, D. A.; Ovens, J. S.; Sigoli, F. A.; Murugesu, M. Room-Temperature Upconversion in a Nanosized {Ln15} Molecular Cluster-Aggregate. *ACS Nano* **2021**, *15* (3), 5580–5585.

(19) Knighton, R. C.; Soro, L. K.; Lecointre, A.; Pilet, G.; Fateeva, A.; Pontille, L.; Francés-Soriano, L.; Hildebrandt, N.; Charbonnière, L. J. Upconversion in Molecular Hetero-Nonanuclear Lanthanide Complexes in Solution. *Chem. Commun.* **2021**, *57* (1), 53–56.

(20) Galico, D.A.; Murugesu, M. Lifetime thermometry with an ytterbium(III)–terbium(III) molecular upconverter. *J. Mater. Chem. C*, **2024**, *12*, 15413-15417.

(21) Gálico, D.A.; Ramdani, R.; Murugesu, M. Phonon-assisted molecular upconversion in a holmium(III)-based molecular cluster-aggregate. *Nanoscale*, **2022**, *14*, 9675-9680.

(22) Wang, J.; Jiang, Y.; Liu, J.; Xu, H.; Zhang, Y.; Peng, X.; Kurmoo, M.; Ng, S. W.; Zeng, M. Discrete Heteropolynuclear Yb/Er Assemblies: Switching on Molecular Upconversion Under Mild Conditions. *Angew. Chem. Int. Ed.* **2021**, *60* (41), 22368–22375.

(23) Zare, D.; Suffren, Y.; Guénée, L.; Eliseeva, S. V.; Nozary, H.; Aboshyan-Sorgho, L.; Petoud, S.; Hauser, A.; Piguet, C. Smaller than a Nanoparticle with the Design of Discrete Polynuclear Molecular Complexes Displaying Near-Infrared to Visible Upconversion. *Dalton Trans.* **2015**, *44* (6), 2529–2540.

(24) Balashova, T. V.; Pushkarev, A. P.; Yablonskiy, A. N.; Andreev, B. A.; Grishin, I. D.; Rumyantcev, R. V.; Fukin, G. K.; Bochkarev, M. N. Organic Er-Yb Complexes as Potential Upconversion Materials. *J. Lumin.* **2017**, *192*, 208–211.

(25) Monteiro, J. H. S. K.; Hiti, E. A.; Hardy, E. E.; Wilkinson, G. R.; Gorden, J. D.; Gorden, A. E. V.; Bettencourt-Dias, A. de. New Up-Conversion Luminescence in Molecular Cyano-Substituted Naphthylsalophen Lanthanide(III) Complexes. *Chem. Commun.* **2021**, *57* (20), 2551–2554.

(26) Hyppänen, I.; Lahtinen, S.; Ääritalo, T.; Mäkelä, J.; Kankare, J.; Soukka, T. Photon Upconversion in a Molecular Lanthanide Complex in Anhydrous Solution at Room Temperature. *ACS Photonics* **2014**, *1* (5), 394–397.

(27) Soro, L. K.; Knighton, R. C.; Avecilla, F.; Thor, W.; Przybilla, F.; Jeannin, O.; Esteban-Gomez, D.; Platas-Iglesias, C.; Charbonnière, L. J. Solution-State Cooperative Luminescence Upconversion in Molecular Ytterbium Dimers. *Adv. Opt. Mater.* **2023**, *11* (11), 2202307.

(28) Salley, G. M.; Valiente, R.; Guedel, H. U. Luminescence Upconversion Mechanisms in Yb^{3+}–Tb^{3+} Systems. *J. Lumin.* **2001**, *94–95*, 305–309.

(29) Salley, G. M.; Valiente, R.; Güdel, H. U. Phonon-Assisted Cooperative Sensitization of Tb^{3+} in $SrCl_2$:Yb, Tb. *J. Phys. Condens. Matter* **2002**, *14* (22), 5461.

(30) Puchalska, M.; Zych, E.; Sobczyk, M.; Watras, A.; Deren, P. Cooperative energy transfer in Yb^{3+}-Tb^{3+} co-doped $CaAl_4O_7$ upconverting phosphor. *Mater. Chem. Phys.* **2015**, *156*, 220-226.

(31) Mo, J.-T.; Wang, Z.; Fu, P.-Y.; Zhang, L.-Y.; Fan, Y.-N.; Pan, M.; Su, C.-Y. Highly Efficient DCL, UCL, and TPEF in Hybridized Ln-Complexes from Ir-Metalloligand. *CCS Chem.* **2020**, *3* (2), 729–738.

(32) Kalmbach, J.; Wang, C.; You, Y.; Förster, C.; Schubert, H.; Heinze, K.; Resch-Genger, U.; Seitz, M. Near-IR to Near-IR Upconversion Luminescence in Molecular Chromium Ytterbium Salts. *Angew. Chem. Int. Ed.* **2020**, *59* (42), 18804–18808.

(33) Knighton, R. C.; Soro, L. K.; Thor, W.; Strub, J.-M.; Cianférani, S.; Mély, Y.; Lenertz, M.; Wong, K.-L.; Platas-Iglesias, C.; Przybilla, F.; Charbonnière, L. J. Upconversion in a d–f [RuYb3] Supramolecular Assembly. *J. Am. Chem. Soc.* **2022**, *144* (29), 13356–13365.

(34) Cevallos-Toledo, R. B.; Bellezza, D.; Ferrera-González, J.; Giussani, A.; Ortí, E.; González-Béjar, M.; Pérez-Prieto, J. Cooperative Sensitization Upconversion in Ytterbium(III)-Based Eosin Lake Pigments. *Chem. Photo. Chem* **2023**, *7* (10), e202300156.

(35) Kiseleva, N.; Nazari, P.; Dee, C.; Busko, D.; Richards, B. S.; Seitz, M.; Howard, I. A.; Turshatov, A. Lanthanide Sensitizers for Large Anti-Stokes Shift Near-Infrared-to-Visible Triplet–Triplet Annihilation Photon Upconversion. *J. Phys. Chem. Lett.* **2020**, *11* (7), 2477–2481.

(36) Qin, W.P.; Liu, Z.Y.; Sin, C.N.; Wu, C.F.; Qin, G.S.; Chen, Z.; Zheng, K.Z. Multi-ion cooperative processes in Yb^{3+} clusters. *Light Sci Appl* **2014**, *3*, e193.

(37) Nakazawa, E. Cooperative optical transitions of Yb^{3+}-Yb^{3+} and Gd^{3+}-Yb^{3+} ion pairs in $YbPO_4$ hosts. J. Lumin. **1976**, 12, 675-680.

(38) Nonat, A.; Bahamyirou, S.; Lecointre, A.; Przybilla, F.; Mély, Y.; Platas-Iglesias, C.; Camerel, F.; Jeannin, O.; Charbonnière, L. J. Molecular Upconversion in Water in Heteropolynuclear Supramolecular Tb/Yb Assemblies. *J. Am. Chem. Soc.* **2019**, *141* (4), 1568–1576.

(39) Hu, J.-Y.; Ning, Y.; Meng, Y.-S.; Zhang, J.; Wu, Z.-Y.; Gao, S.; Zhang, J.-L. Highly Near-IR Emissive Ytterbium(III) Complexes with Unprecedented Quantum Yields. *Chem. Sci.* **2017**, *8* (4), 2702–2709.

(40) Gálico, D. A.; Ramdani, R.; Murugesu, M. Phonon-Assisted Molecular Upconversion in a Holmium(III)-Based Molecular Cluster-Aggregate. *Nanoscale* **2022**, *14* (27), 9675–9680.

(41) Comby, S.; Bünzli, J.-C. G. Chapter 235 Lanthanide Near-Infrared Luminescence in Molecular Probes and Devices. In *Handbook on the Physics and Chemistry of Rare Earths*; Gschneidner, K. A., Bünzli, J.-C., Pecharsky, V. K., Eds.; Elsevier, 2007; Vol. 37, pp 217–470.

(42) Mickert, M.J.; Farka, Z.; Kostiv, U.; Hlaváček, A.; Horák, D.; Skládal, P.; Gorris, H.H. Measurement of sub-femtomolar concentrations of prostate-specific antigen through single-molecule counting with an upconversion-linked immunosorbent assay. *Anal. Chem.* **2019**, *91*, 9435-9441.

(43) Dukhno, O.; Ghosh, S. ; Greiner, V. ; Bou, S. ; Godet, J. ; Muhr, V. ; Buchner, M.; Hirsch, T.; Mély, Y.; Przybilla, F. Targeted single particle tracking with upconverting nanoparticles. *ACS Appl. Mater. Interfaces* **2024**, 16, 11217–11227.

(44) Dukhno, O.; Przybilla, F.; Muhr, V.; Buchner, M.; Hirsch, T.; Mély, Y. Time-Dependent Luminescence Loss for Individual Upconversion Nanoparticles upon Dilution in Aqueous Solution. *Nanoscale* **2018**, *10* (34), 15904–15910.

(45) Lahtinen, S.; Lyytikäinen, A.; Päkkilä, H.; Hömppi, E.; Perälä, N.; Lastusaari, M.; Soukka, T. Disintegration of Hexagonal $NaYF_4$:Yb^{3+},Er^{3+} Upconverting Nanoparticles in Aqueous Media: The Role of Fluoride in Solubility Equilibrium. *J. Phys. Chem. C* **2017**, *121* (1), 656–665.

(46) Gnach, A.; Lipinski, T.; Bednarkiewicz, A.; Rybka, J.; Capobianco, J. A. Upconverting Nanoparticles: Assessing the Toxicity. *Chem. Soc. Rev.* **2015**, *44* (6), 1561–1584.

(47) Souri, N.; Tian, P.; Lecointre, A.; Lemaire, Z.; Chafaa, S.; Strub, J.-M.; Cianférani, S.; Elhabiri, M.; Platas-Iglesias, C.; Charbonnière, L. J. Step by Step Assembly of Polynuclear Lanthanide Complexes with a Phosphonated Bipyridine Ligand. *Inorg. Chem.* **2016**, *55* (24), 12962–12974.

(48) Souri, N.; Tian, P.; Platas-Iglesias, C.; Wong, K.-L.; Nonat, A.; Charbonnière, L. J. Upconverted Photosensitization of Tb Visible Emission by NIR Yb Excitation in Discrete Supramolecular Heteropolynuclear Complexes. *J. Am. Chem. Soc.* **2017**, *139* (4), 1456–1459.

(49) Salaam, J.; Tabti, L.; Bahamyirou, S.; Lecointre, A.; Hernandez Alba, O.; Jeannin, O.; Camerel, F.; Cianférani, S.; Bentouhami, E.; Nonat, A. M.; Charbonnière, L. J. Formation of Mono- and Polynuclear Luminescent Lanthanide Complexes Based on the Coordination of Preorganized Phosphonated Pyridines. *Inorg. Chem.* **2018**, *57* (10), 6095–6106.

(50) André, N.; Jensen, T.B.; Scopelliti, R.; Imbert, D.; Elhabiri, M.; Hopfgartner, G.; Piguet, C.; Bünzli, J.-C.G. Supramolecular recognition of heteropairs of lanthanide ions: a step toward self-assembled bifunctional probes. *Inorg. Chem.* **2004**, *43*, 515–529.

(51) Placidi, M.P.; Villaraza, A.J.L.; Natrajan, L.S.; Sykes, D.; Kenwright, A.M.; Faulkner, S. Synthesis and Spectroscopic Studies on Azo-Dye Derivatives of Polymetallic Lanthanide Complexes: Using Diazotization to Link Metal Complexes Together. *J. Am. Chem. Soc.* **2009**, *131*, 9916–9917.

(52) Natrajan, L.S.; Villaraza, A.J.L.; Kenwright, A.M.; Faulkner, S. Controlled preparation of a heterometallic lanthanide complex containing different lanthanides in symmetrical binding pockets. *Chem. Commun.* **2009**, 6020–6022.

(53) Tremblay, M.S.; Sames, D. Synthesis of luminescent heterometallic bis-lanthanide complexes via selective, sequential metalation. *Chem. Commun.* **2006**, 4116–4118.

(54) Prodi, L.; Montalti, M. ; Zaccheroni, N. ; Pickaert, G.; Charbonnière, L.; Ziessel, R. New europium(iii) complexes containing hybrid ligands with hard and soft complexation centres. *New J. Chem.*, **2003**, *27*, 134–139.

(55) Hamon, N.; Godec, L.; Sanchez, S.; Beyler, M.; Charbonnière, L.J. ; Tripier, R. Upconversion luminescence with Bis-pyclen Yb(III) Chelates: Crown vs. Linear Polyether Linkers in Discrete Heteropolynuclear Architectures *Angew. Chem. Int. Ed.*, **2024**, e202414608.

(56) Hamon, N.; Godec, L.; Jourdain, E.; Lucio-Martínez, F.; Platas-Iglesias, C.; Beyler, M.; Charbonnière, L. J.; Tripier, R. Synthesis and Photophysical Properties of Lanthanide Pyridinylphosphonic Tacn and Pyclen Derivatives: From Mononuclear Complexes to Supramolecular Heteronuclear Assemblies. *Inorg. Chem.* **2023**, *62* (46), 18940–18954.

(57) Hirashima, Y.; Ito, K.; Shiokawa, J. Lanthanoid Chloride Complexes with Polyethylene Glycols and Glymes. Chem. Lett. **1983**, 12 (1), 9–10.

(58) Hirashima, Y.; Shiokawa, J. Crystalline Complexes of Poly(Oxyethylene) Derivatives with Lanthanoids. *Chem. Lett.* **1979**, *8* (5), 463–464.

(59) Bünzli, J.-C. G.; Wessner, D. Rare Earth Complexes with Neutral Macrocyclic Ligands. *Coord. Chem. Rev.* **1984**, *60*, 191–253.

(60) Z. Kokan, M.J. Chmielewski, A photoswitchable heteroditopic ion-pair rReceptor J. Am. Chem. Soc. 2018, 140, 16010-16014.

(61) Mameri, S.; Charbonnière, L.J.; Ziessel, R. F. Lanthanide/ATP interaction in water mediated by luminescent hemispherical-shaped complexes *Inorg. Chem.* **2004**, *43*, 1819-1821.

(62) a) Gampp, H.; Maeder, M; Meyer, C. J.; Zuberbühler, A. D. Calculation of equilibrium constants from multiwavelength spectroscopic data—III: Model-free analysis of spectrophotometric and ESR titrations *Talanta* **1985**, *32*, 1133–1139.

(63) Maeder, M.; Zuberbuehler, A. D. Nonlinear Least-Squares Fitting of Multivariate Absorption Data *Anal. Chem.* **1990**, *62*, 2220–2224.

(64) Shannon, R.D. Revised effective ionic radii and systematic studies of interatomic distances in halides and chalcogenides, *Acta Cryst.* **1976**, *A32*, 751-767.

(65) Renaud, F., Piguet, C., Bernardinelli, G., Bünzli, J.-C.G. and Hopfgartner, G. In Search for Mononuclear Helical Lanthanide Building Blocks with Predetermined Properties: Triple-stranded Helical Complexes with N,N,N',N'-tetraethylpyridine-2,6-dicarboxamide. *Chem. Eur. J.*, **1997**, *3*, 1646-1659.

(66) Ishida, H.; Tobita, S.; Hasegawa, Y.; Katoh, R.; Nozaki, K. Recent advances in instrumentation for absolute emission quantum yield measurements *Coord. Chem. Rev.* **2010**, *254*, 2449–2458.

(67) Olmsted, J. Calorimetric determinations of absolute fluorescence quantum yields. *J. Phys. Chem.* **1979**, *83*, 2581–2584.

(68) Benson, R. C.; Kues, H. A Fluorescence properties of indocyanine green as related to angiography. *Phys. Med. Biol.* **1978**, *23*, 159-163.

(69) Weissman, S.I. Intramolecular energy transfer. The fluorescence of complexes of europium. *J. Chem. Phys.* **1942**, *10*, 214-217.

(70) Horrocks, W. DeW.; Sudnick, D.R. Lanthanide ion probes of structure in biology. Laser-induced luminescence decay constants provide a direct measure of the number of metal-coordinated water molecules. *J. Am. Chem. Soc.* **1979**, *101*, 2, 334–340.

(71) Nocton, G.; Nonat, A.; Gateau, C.; Mazzanti, M. Water stability and luminescence of lanthanide complexes of tripodal ligands derived from 1,4,7-triazacyclononane: pyridinecarboxamide versus pyridinecarboxylate donors. *Helv. Chim. Acta*, **2009**, *92*, 2257-2273.

(72) Popov, K.; Rönkkömäki, H.; Lajunen, L.H.J. Critical evaluation of stability constants of phosphonic acids. *Pure Appl. Chem.*, **2001**, 73, 1641–1677.

(73) Ichikawa, T.; Sawada, K. Protonation behavior and intramolecular interactions of alpha,omega-alkanediaminepolymethylenepolyphosphonates. *Bull. Chem. Soc. Jpn* **1997**, *70*, 829-835.

(74) Piguet, C.; Bünzli, J.-C. G.; Bernardinelli, G.; Hopfgartner, G.; Williams, A.F. Self-assembly and photophysical properties of lanthanide dinuclear triple-helical complexes. *J. Am. Chem. Soc.* **1993**, *115*, 8197–8206.

(75) Vergeer, P.; Vlugt, T. J. H.; Kox, M. H. F.; den Hertog, M. I.; van der Eerden, J.; Meijerink, A. Quantum cutting by cooperative energy transfer in $Yb_xY_{1-x}PO_4$:Tb^{3+}. *Phys. Rev. B* **2005**, *71*, 014119.

(76) Pini, F.; Knighton, R.C.; Soro, L.K.; Charbonnière, L.J.; Natile, M.N.; Hildebrandt, N. Equal Rights for Activators - Ytterbium to Terbium Cooperative Sensitization in Molecular Upconversion. *Adv. Opt. Mater*. **2024**, 2400423.

(77) Pollnau, M.; Gamelin, D. R.; Lüthi, S. R.; Güdel, H. U.; Hehlen, M.P. Power dependence of upconversion luminescence in lanthanide and transition-metal-ion systems. *Phys. Rev. B.* **2000**, *61*, 3337-3346.

(78) Patiny, L.; Borel, A. ChemCalc: A building block for tomorrow's chemical infrastructure. *J. Chem. Inf. Model.* **2013**, *53*, 5, 1223–1228.

(79) Jones, C.M.S.; Gakamsky, A.; Marques-Hueso The upconversion quantum yield (UCQY): a review to standardize the measurement methodology, improve comparability, and define efficiency standards. *Sci Tech. Adv. Mater.* **2021**, *22*, 810-848.

(80) Naseri, S.; Taarit, I.; Bolvin, H.; Bünzli, J. C.-G.; Fürstenberg, A.; Guénée, L.; Le-Hoan, G.; Mirzakhani, M.; Nozary, H.; Rosspeintner, A.; Piguet, C. Symmetry and Rigidity for Boosting Erbium-Based Molecular Light-Upconversion in Solution. *Angew. Chem. Int. Ed. Engl* **2023**, 62, e202314503.

.